

Numerical Analysis of a Bio-Polymerization Model

Ali Balooch^a, Faranak Courtney-Pahlevani^b, Lisa Davis^c, Adrian Dunca^d,
Monika Neda^a, Jorge Reyes^{e,*}

^a*Department of Mathematical Sciences, University of Nevada, Las Vegas, Las Vegas, Box
454020, NV, USA*

^b*Division of Science & Engineering, Penn State University - Abington, Abington
, 19001, PA, USA*

^c*Department of Mathematical Sciences, Montana State University, Bozeman, Box
172400, MT, USA*

^d*Department of Mathematics and Informatics, Politehnica University of
Bucharest, Bucharest, Romania*

^e*Department of Mathematics, Virginia Tech, Blacksburg, 24060, VA, USA*

Abstract

This work studies a stabilization technique for first-order hyperbolic differential equations used in DNA transcription modeling. Specifically we use the Lighthill-Whitham-Richards Model with a nonlinear Greenshield's velocity proposed in [1]. Standard finite element methods are known to produce spurious oscillations when applied to nonsmooth solutions. To address this, we incorporate stabilization terms involving spatial and temporal filtering into the system. We present numerical stability and prove convergence results for both the backwards Euler and time filtered formulations. We also present several computational results to demonstrate the rates in space and in time as well as for selected biological scenarios.

Keywords: Lighthill-Whitham-Richards Model, Greenshield's velocity model, finite element, DNA transcription,

PACS: 02.60.-x, 02.60.Cb, 87.10.Ed, 87.15.Aa

2020 MSC: 65M12, 65M60, 92-08, 92-10

*Corresponding author

Email addresses: `ali.balooch@unlv.edu` (Ali Balooch), `fxp10@psu.edu` (Faranak Courtney-Pahlevani), `lisa.davis@montana.edu` (Lisa Davis), `argus_adrian.dunca@upb.ro` (Adrian Dunca), `monika.neda@unlv.edu` (Monika Neda), `reyesj@vt.edu` (Jorge Reyes)

URL: `http://neda.faculty.unlv.edu/` (Monika Neda)

1. Introduction

This paper describes the analysis of a simulation framework for a comprehensive model of ribosome abundance control in bacteria. The full model combines a mathematical description of bio-polymerization processes: *transcription* of ribosomal RNA, transcription of *messenger RNA* (mRNA) of ribosomal proteins (r-proteins) and *translation* of r-proteins with a characterization of feedback mechanisms that regulate initiation rates, processing rates and abundance of key molecules. Here we focus on the prototype for each of the compartment models describing the processes of transcription and translation. These processes are fundamentally characterized by the motion of a molecular motor copying a segment of DNA or mRNA. The speed at which these motors travel along the strand while reading the gene is referred to as the *elongation velocity*, and in the authors' previous work [1–3], the LWR model with the Greenshield's velocity is used for each compartment. The model is useful for describing the situation where many motors are copying the segment simultaneously. In such cases, the elongation velocities can be non-uniform, resulting in significant variations in the density of the molecular motors in different spatial regions of the DNA segment. For a comprehensive description of the model development, the reader is referred to [1] and the references therein.

The LWR with the Greenshield's model [4] is given by

$$\frac{\partial \rho}{\partial t} + \left(v_f - \frac{2v_f}{\rho_m} \rho \right) \frac{\partial \rho}{\partial x} = 0, \quad (1)$$

where v_f is the free flow speed and ρ_m is the maximum jam density. The free flow speed v_f represents the speed of the traffic when the density ρ is zero. The maximum density ρ_m is the traffic density at which the speed of traffic v is equal to zero.

It is known that when we solve the hyperbolic partial differential equation (PDE) given by equation (1), oscillations exist around the shock solutions. Herein, we apply a stabilization of finite element method (FEM) introduced in [5] for the advection equation based on Vreman filtering [6]. Additionally, we use a simple time filter first introduced in [7]. This time filter does not add computational complexity and is shown to be second order accurate in time [7, 8].

In [9] the time filter is shown to be effective at improving accuracy when combined with an explicit first order upwind finite difference method with minimal expense in numerical implementation for the linear advection equation case. There the filtered scheme introduces a small amount of dissipation into the behavior of a non-smooth solution, thereby increasing accuracy while preventing spurious oscillations.

The remainder of the paper is organized as follows. Section 2 has notation, preliminaries, and algorithms. Section 3 presents numerical results for the stability and convergence analysis of the model, followed by computational experiments in Section 4. We conclude our work in Section 5.

2. Notation, Preliminaries and Algorithms

Let the interval $\Omega \subset \mathbb{R}$ denote the domain, while the $L^2(\Omega)$ norm and the inner product are denoted by $\|\cdot\|$ and (\cdot, \cdot) respectively. The norm of the $H^k(\Omega)$ space is denoted by $\|\cdot\|_k$. The analysis is carried out in the periodic setting. Thus, the function space used is $X := H^1_{\#}(\Omega)$, which is the closure of the C^∞ periodic functions in Ω in the H^1 norm. Let $X_h \subset X$ be the subspace of finite elements.

The continuous mean $\bar{u} \in X$ of $u \in X$ is the solution of the PDE [10],

$$-\delta^2 \Delta \bar{u} + \bar{u} = u.$$

We denote $G : L^2(\Omega) \rightarrow X$ as the filtering operator, i.e. $G(u) = \bar{u}$. Furthermore, we consider the discrete mean $\bar{u}^h \in X_h$ of $u \in X$, defined as the unique solution of

$$\delta^2 (\nabla \bar{u}^h, \nabla v_h) + (\bar{u}^h, v_h) = (u, v_h), \quad \forall v_h \in X_h,$$

where the mean quantities are associated with the filtering length scale δ [11]. We denote the discrete filtering operator as $G_h : L^2(\Omega) \rightarrow X_h$, where $G_h(u) = \bar{u}^h$. Next, we define the deconvolution operators,

Definition 2.1. *The N^{th} order van Cittert continuous and discrete deconvolution operators as $D_N : X \mapsto X$ and $D_N^h : X \rightarrow X_h$ are, respectively,*

$$D_N := \sum_{n=0}^N (I - G)^n, \quad \text{and} \quad D_N^h := \sum_{n=0}^N (I - G_h)^n.$$

The stability and accuracy properties of continuous and discrete averaging and deconvolution have been studied in [11–16]. The operators denoted as $\bar{\cdot}$ and $\bar{\cdot}^h$ represent filtering and lend the physical meaning to the parameter δ as the filter width. In general, in the finite element setting, δ depends on the mesh size denoted by h .

We present several properties and lemmas used in our analysis below.

Lemma 2.1 (Smoothing Property [17]). *For any $u_h \in X_h$,*

$$\delta^2 \|\Delta^h (D_N^h \bar{u}_h^h)\| + \delta \|\nabla (D_N^h \bar{u}_h^h)\| + \|D_N^h \bar{u}_h^h\| \leq C(N) \|u_h\| ,$$

where Δ^h is the discrete Laplacian operator and $C(N)$ is a generic constant that depends on the order of deconvolution N .

Lemma 2.2 (Deconvolution error estimate [5]). *There exist general constants $C, C(N)$ such that for all $u \in X \cap H^{2N+2}(\Omega) \cap H^{k+1}$,*

$$\delta \|\nabla u - \nabla D_N^h \bar{u}^h\| \leq C(N)(\delta h^k + h^{k+1}) \|u\|_{k+1} + C\delta^{2N+3} \|\nabla u\|_{2N+3} .$$

Additionally, we assume the following approximation properties, [18, 19]:

$$\inf_{v \in X_h} \|u - v\| \leq Ch^{k+1} \|u\|_{k+1}, \quad u \in H^{k+1}(\Omega), \quad (2)$$

$$\inf_{v \in X_h} \|\nabla(u - v)\| \leq Ch^k \|u\|_{k+1}, \quad u \in H^{k+1}(\Omega). \quad (3)$$

There exists an interpolant I_h of u as constructed by Brenner and Scott [18] so that (2) and (3) hold with I_h instead of v . We will apply the approximation property 4.4.25 with $p = \infty, m = 2, s = 1, l = 0, n = 1$ on page 110, where l is defined as in Lemma 4.4.41 in [18]. Thus, I_h approximates u in the norm of the Sobolev space W_∞^1 in the order of h . Due to these approximation properties of the interpolant I_h , it follows that if $\left\| \frac{\partial^2 u}{\partial x^2} \right\|_{L^\infty} < C$ then both terms below are bounded uniformly for $h < 1$, i.e.

$$\left\| \frac{\partial I_h}{\partial x} \right\|_{L^\infty}, \left\| \frac{\partial(u - I_h)}{\partial x} \right\|_{L^\infty} < C.$$

Lemma 2.3 is a convenient algebraic identity from [8] which will be used in a similar manner for the convergence analysis.

Lemma 2.3. *The following identity holds*

$$\begin{aligned} & \left(\frac{3}{2}a - 2b + \frac{1}{2}c\right) \left(\frac{3}{2}a - b + \frac{1}{2}c\right) = \\ & \frac{1}{4}(a^2 + (2a - b)^2 + (a - b)^2) - \frac{1}{4}(b^2 + (2b - c)^2 + (b - c)^2) + \frac{3}{4}(a - 2b + c)^2. \end{aligned}$$

The convergence analysis uses a discrete Gronwall inequality [20] stated below.

Lemma 2.4. *Let Δt , H , and a_n, b_n, c_n, γ_n (for integers $n \geq 0$) be finite nonnegative numbers such that*

$$a_l + \Delta t \sum_{n=0}^l b_n \leq \Delta t \sum_{n=0}^l \gamma_n a_n + \Delta t \sum_{n=0}^l c_n + H \quad \text{for } l \geq 0.$$

Suppose that $\Delta t \gamma_n < 1 \forall n$. Then,

$$a_l + \Delta t \sum_{n=0}^l b_n \leq \exp \left(\Delta t \sum_{n=0}^l \frac{\gamma_n}{1 - \Delta t \gamma_n} \right) \left(\Delta t \sum_{n=0}^l c_n + H \right) \quad \text{for } l \geq 0.$$

Next we introduce the variational formulation for the LWR model with Greenshield's velocity and Vreman stabilization term. Find $\rho_h \in X_h$ satisfying for all $v \in X_h$

$$\left(\frac{\partial}{\partial t} \rho_h, v_h \right) + v_f \left(\frac{\partial}{\partial x} \rho_h, v_h \right) - \frac{2v_f}{\rho_m} b(\rho_h, \rho_h, v_h) + \chi \delta^2 \left(\frac{\partial}{\partial x} \rho_h^*, \frac{\partial}{\partial x} v_h^* \right) = 0,$$

where the stabilization term $\chi \delta^2 \left(\frac{\partial}{\partial x} \rho^*, \frac{\partial}{\partial x} v_h^* \right)$, initially introduced by Vreman [6] is added. Here $\rho^* = \rho - D_N^h \bar{\rho}^h$ and the goal of this term is to improve accuracy and damp unwanted spurious oscillations. This also introduces the dimensionless χ as a stabilization parameter which can be manually tuned to increase or decrease the effects of the added stabilization term. Based on [21] we also define trilinear term $b(\cdot, \cdot, \cdot) : X \times X \times X \rightarrow \mathbb{R}$ as

$$b(u, v, w) = \frac{1}{3} \int_{\Omega} \left(\frac{\partial}{\partial x} (uv) + u \frac{\partial v}{\partial x} \right) w \, dx. \quad (4)$$

In [21, 22] it is proven that b is skew-symmetric, i.e.

$$b(u, v, w) + b(u, w, v) = 0. \quad (5)$$

We also use the following lemma.

Lemma 2.5. *For $u, v, w \in X$ we have the following identities*

$$b(u, v, w) = \frac{1}{3} \int_{\Omega} u \frac{\partial v}{\partial x} w dx - \frac{1}{3} \int_{\Omega} v \frac{\partial w}{\partial x} u dx, \quad (6)$$

$$b(u, v, w) = -\frac{1}{3} \int_{\Omega} v \frac{\partial u}{\partial x} w dx - \frac{2}{3} \int_{\Omega} v \frac{\partial w}{\partial x} u dx, \quad (7)$$

$$2 \int_{\Omega} u \frac{\partial v}{\partial x} v dx = - \int_{\Omega} v \frac{\partial u}{\partial x} v dx. \quad (8)$$

Proof. From (4) we have that

$$b(u, v, w) = \frac{2}{3} \int_{\Omega} u \frac{\partial v}{\partial x} w dx + \frac{1}{3} \int_{\Omega} v \frac{\partial u}{\partial x} w dx. \quad (9)$$

Applying integration by parts on the second term results in (9) becoming

$$\begin{aligned} b(u, v, w) &= \frac{2}{3} \int_{\Omega} u \frac{\partial v}{\partial x} w dx - \frac{1}{3} \int_{\Omega} u \frac{\partial}{\partial x} (vw) dx \\ &= \frac{1}{3} \int_{\Omega} u \frac{\partial v}{\partial x} w dx - \frac{1}{3} \int_{\Omega} v \frac{\partial w}{\partial x} u dx. \end{aligned}$$

To prove (7) we just apply integration by parts on the first term of (9) instead giving

$$\begin{aligned} b(u, v, w) &= -\frac{2}{3} \int_{\Omega} v \frac{\partial}{\partial x} (uw) dx + \frac{1}{3} \int_{\Omega} v \frac{\partial u}{\partial x} w dx \\ &= -\frac{1}{3} \int_{\Omega} v \frac{\partial u}{\partial x} w dx - \frac{2}{3} \int_{\Omega} v \frac{\partial w}{\partial x} u dx. \end{aligned}$$

Lastly, to prove (8) consider

$$2 \int_{\Omega} u \frac{\partial v}{\partial x} v dx = \int_{\Omega} u \frac{\partial}{\partial x} (v^2) dx = - \int_{\Omega} v \frac{\partial u}{\partial x} v dx$$

□

Lastly, let Δt denote the time step, then $t^n = n\Delta t$, $n = 0, 1, \dots, M$, and final time is $T := M\Delta t$. Here, and in the sequel we adopt the notation $u(t^n, \cdot) = u^n$

$$\| \| u \| \|_{\infty, k} := \max_{0 \leq n \leq M} \| u^n \|_k, \quad \| \| u \| \|_{m, k} := \left(\Delta t \sum_{n=0}^M \| u^n \|_k^m \right)^{1/m}.$$

2.1. Algorithms

We study two algorithms. First we employ the backward Euler temporal discretization which gives the following algorithm.

Algorithm 2.1. For $n = 1, 2, \dots, M$ find $\rho_h^n \in X_h$ such that,

$$\begin{aligned} \frac{1}{\Delta t} (\rho_h^n - \rho_h^{n-1}, v_h) + v_f \left(\frac{\partial}{\partial x} \rho_h^n, v_h \right) - \frac{2v_f}{\rho_m} b(\rho_h^n, \rho_h^n, v_h) \\ + \chi \delta^2 \left(\frac{\partial}{\partial x} \rho_h^{n*}, \frac{\partial}{\partial x} v_h^* \right) = 0, \quad \forall v_h \in X_h. \end{aligned} \quad (10)$$

We also implement the time filter studied in [7, 8, 23] as a post-processing step, which yields the following algorithm.

Algorithm 2.2. For $n = 2, 3, \dots, M$ find $\rho_h^n \in X_h$ such that,

Step 1: Backward Euler

$$\begin{aligned} \frac{1}{\Delta t} (\hat{\rho}_h^n - \rho_h^{n-1}, v_h) + v_f \left(\frac{\partial}{\partial x} \hat{\rho}_h^n, v_h \right) - \frac{2v_f}{\rho_m} b(\hat{\rho}_h^n, \hat{\rho}_h^n, v_h) \\ + \chi \delta^2 \left(\frac{\partial}{\partial x} \hat{\rho}_h^{n*}, \frac{\partial}{\partial x} v_h^* \right) = 0, \quad \forall v_h \in X_h, \end{aligned} \quad (11)$$

Step 2: Time Filter

$$\rho_h^n = \hat{\rho}_h^n - \frac{\gamma}{2} (\hat{\rho}_h^n - 2\rho_h^{n-1} + \rho_h^{n-2}).$$

Algorithm 2.2 approximates the density ρ^n from the intermediate density approximation from step 1, i.e. $\hat{\rho}^n$. This increases the convergence rate in time from first to second order.

By choosing $\gamma = \frac{2}{3}$ in the time filter equation in step 2 we obtain for $\hat{\rho}_h^n$ the following,

$$\hat{\rho}_h^n = \frac{3}{2} \rho_h^n - \rho_h^{n-1} + \frac{1}{2} \rho_h^{n-2}. \quad (12)$$

Replacing $\hat{\rho}_h^n$ in step 1 by (12), one can reduce the two step process to a single equation. For simplicity in notation, we introduce the interpolation

and difference operators as

$$I[u^n] = \frac{3}{2}u^n - u^{n-1} + \frac{1}{2}u^{n-2}, \text{ and} \quad (13)$$

$$D[u^n] = \frac{3}{2}u^n - 2u^{n-1} + \frac{1}{2}u^{n-2}, \quad (14)$$

as well as

$$\mathcal{E}[u^n] = \frac{1}{4} \left(\|u^n\|^2 + \|2u^n - u^{n-1}\|^2 + \|u^n - u^{n-1}\|^2 \right), \quad (15)$$

$$\mathcal{Z}[u^n] = \frac{3}{4} \|u^n - u^{n-1} - u^{n-2}\|^2, \quad (16)$$

which are used in the analysis of Algorithm 2.2.

Incorporating (13) and (14) into Algorithm 2.2 and using (12), we obtain the following equivalent scheme

$$\begin{aligned} \frac{1}{\Delta t} (D[\rho_h^n], v_h) + v_f \left(\frac{\partial}{\partial x} I[\rho_h^n], v_h \right) - \frac{2v_f}{\rho_m} b(I[\rho_h^n], I[\rho_h^n], v_h) \\ + \chi \delta^2 \left(\frac{\partial}{\partial x} I[\rho_h^n]^*, \frac{\partial}{\partial x} v_h^* \right) = 0. \end{aligned} \quad (17)$$

The initial condition ρ_h^0 is the L^2 projection of ρ_0 and ρ_h^1 is obtained using backward Euler.

Lemma 2.6 ([8]). *For u sufficiently smooth, we have*

$$\left\| \frac{D[u(t^{n+1})]}{\Delta t} - u_t(t^{n+1}) \right\|^2 \leq \frac{6}{5} \Delta t^3 \int_{t^{n-1}}^{t^{n+1}} \|u_{ttt}\|^2 dt, \quad (18)$$

$$\|I[u(t^{n+1})] - u(t^{n+1})\|^2 \leq \frac{4}{3} \Delta t^3 \int_{t^{n-1}}^{t^{n+1}} \|u_{tt}\|^2 dt. \quad (19)$$

3. Numerical Analysis

First we present the numerical stability of our algorithms followed by convergence theorems.

Lemma 3.1. *Solutions to the fully discrete Algorithm 2.1 are unconditionally stable and satisfy*

$$\|\rho_h^M\|^2 + 2\chi\delta^2\Delta t \sum_{n=1}^M \left\| \frac{\partial}{\partial x} \rho_h^{n*} \right\|^2 \leq \|\rho_0\|^2.$$

Proof. Setting $v_h = \rho_h^n$ in (10) yields

$$\frac{1}{\Delta t} \|\rho_h^n\|^2 - \frac{1}{\Delta t} (\rho_h^{n-1}, \rho_h^n) + \chi \delta^2 \left\| \frac{\partial}{\partial x} \rho_h^{n*} \right\|^2 = -v_f \left(\frac{\partial}{\partial x} \rho_h^n, \rho_h^n \right) + \frac{2v_f}{\rho_m} b(\rho_h^n, \rho_h^n, \rho_h^n). \quad (20)$$

The first term on the right-hand side vanishes due to the periodicity of functions in X_h , as

$$\left(\frac{\partial}{\partial x} \rho_h^n, \rho_h^n \right) = \frac{1}{2} \int_{\Omega} \frac{\partial}{\partial x} (\rho_h^n)^2 dx = 0.$$

Since the trilinear term $b(\cdot, \cdot, \cdot)$ is skew-symmetric by (5), the other term on the right-hand side also vanishes. Note that applying Cauchy-Schwarz inequality and Young's inequality in succession gives

$$-\frac{1}{\Delta t} (\rho_h^{n-1}, \rho_h^n) \geq -\frac{1}{2\Delta t} \|\rho_h^{n-1}\|^2 - \frac{1}{2\Delta t} \|\rho_h^n\|^2.$$

Then (20) becomes

$$\frac{1}{2\Delta t} \|\rho_h^n\|^2 - \frac{1}{2\Delta t} \|\rho_h^{n-1}\|^2 + \chi \delta^2 \left\| \frac{\partial}{\partial x} \rho_h^{n*} \right\|^2 \leq 0.$$

Multiplying by $2\Delta t$ and summing $n = 1, 2, \dots, M$ results in

$$\|\rho_h^M\|^2 - \|\rho_h^0\|^2 + 2\chi \delta^2 \Delta t \sum_{n=1}^M \left\| \frac{\partial}{\partial x} \rho_h^{n*} \right\|^2 \leq 0,$$

and recalling that ρ_h^0 is the L^2 projection of ρ_0 completes the proof. \square

From [1] we have the following stability result for Algorithm 2.2 with $\gamma = \frac{2}{3}$.

Lemma 3.2. *The solution to Algorithm 2.2 given by (17) is unconditionally stable and it satisfies*

$$\|\rho_h^M\|^2 + 4 \sum_{n=2}^M \mathcal{Z}[\rho_h^n] + 2\chi \delta^2 \Delta t \sum_{n=2}^M \left\| \frac{\partial}{\partial x} I[\rho_h^n]^* \right\|^2 \leq C(\rho_0, \rho_1), \quad (21)$$

where $\mathcal{Z}[\rho_h^n]$ is defined by (16).

Next, we will study the convergence analysis.

Theorem 3.1. *Let ρ_h^n be the solution of Algorithm 2.1 and ρ be a solution of (1) with enough regularity. Then, for sufficiently small Δt we have*

$$\begin{aligned} & \|\rho^M - \rho_h^M\|_{\infty,0}^2 \leq Ch^{2k+2} \|\rho\|_{\infty,k+1}^2 + CK \left(\chi \delta^{4N+6} \left\| \frac{\partial \rho}{\partial x} \right\|_{2N+3}^2 \right. \\ & \quad + \chi h^{2k+2} \|\rho\|_{2,k+1}^2 + \chi \delta^2 h^{2k} \|\rho\|_{2,k+1}^2 \\ & \quad + \frac{v_f^2}{\delta^2} \left(\frac{1}{\chi} + 1 \right) h^{2k+2} \|\rho\|_{2,k+1}^2 + h^{2k+2} \int_{t^0}^{t^M} \|\rho_t\|_{k+1}^2 dt \\ & \quad \left. + \Delta t^2 \int_{t^0}^{t^M} \|\rho_{tt}\|^2 dt + \frac{v_f^2}{\rho_m^2} \left(1 + \frac{1}{\chi \delta^2} + \frac{1}{\delta^2} \right) h^{2k+2} \|\rho\|_{2,k+1}^2 \right), \end{aligned}$$

where $K = \exp \left(\Delta t \sum_{n=0}^M \frac{\gamma_n}{1 - \Delta t \gamma_n} \right)$ and $\gamma_n = C \left(\frac{v_f}{\rho_m} + 1 \right)$.

Proof. Evaluating the weak formulation of (1) at time t^n yields

$$\begin{aligned} & \frac{1}{\Delta t} (\rho^n - \rho^{n-1}, v_h) + v_f \left(\frac{\partial}{\partial x} \rho^n, v_h \right) - \frac{2v_f}{\rho_m} b(\rho^n, \rho^n, v_h) + \chi \delta^2 \left(\frac{\partial}{\partial x} \rho^{n*}, \frac{\partial}{\partial x} v_h^* \right) \\ & = \left(\frac{\rho^n - \rho^{n-1}}{\Delta t} - \frac{\partial}{\partial t} \rho^n, v_h \right) + \chi \delta^2 \left(\frac{\partial}{\partial x} \rho^{n*}, \frac{\partial}{\partial x} v_h^* \right). \end{aligned}$$

Subtracting (10) from the above equation gives

$$\begin{aligned} & \frac{1}{\Delta t} (e^n - e^{n-1}, v_h) + v_f \left(\frac{\partial}{\partial x} e^n, v_h \right) - \frac{2v_f}{\rho_m} (b(\rho^n, \rho^n, v_h) - b(\rho_h^n, \rho_h^n, v_h)) \\ & + \chi \delta^2 \left(\frac{\partial}{\partial x} e^{n*}, \frac{\partial}{\partial x} v_h^* \right) = \left(\frac{\rho^n - \rho^{n-1}}{\Delta t} - \frac{\partial}{\partial t} \rho^n, v_h \right) + \chi \delta^2 \left(\frac{\partial}{\partial x} \rho^{n*}, \frac{\partial}{\partial x} v_h^* \right), \end{aligned}$$

where $e^n = \rho^n - \rho_h^n$. Rewriting the trilinear terms by adding and subtracting $b(\rho_h^n, \rho^n, v_h)$ yields

$$\begin{aligned} & \frac{1}{\Delta t} (e^n - e^{n-1}, v_h) + v_f \left(\frac{\partial}{\partial x} e^n, v_h \right) - \frac{2v_f}{\rho_m} (b(e^n, \rho^n, v_h) + b(\rho_h^n, e^n, v_h)) \\ & + \chi \delta^2 \left(\frac{\partial}{\partial x} e^{n*}, \frac{\partial}{\partial x} v_h^* \right) = \left(\frac{\rho^n - \rho^{n-1}}{\Delta t} - \frac{\partial}{\partial t} \rho^n, v_h \right) + \chi \delta^2 \left(\frac{\partial}{\partial x} \rho^{n*}, \frac{\partial}{\partial x} v_h^* \right). \end{aligned}$$

Next, we decompose the error as $e^n = \rho^n - I_h^n + I_h^n - \rho_h^n = \eta^n + \phi_h^n$, where I_h^n is the interpolant of ρ^n in X_h as defined in Section 2. We set $v_h = \phi_h^n$ and use $b(\rho_h^n, \phi_h^n, \phi_h^n) = 0$ to obtain

$$\begin{aligned}
& \frac{1}{2\Delta t} \left(\|\phi_h^n\|^2 - \|\phi_h^{n-1}\|^2 \right) + \chi\delta^2 \left\| \frac{\partial}{\partial x} \phi_h^{n*} \right\|^2 = \\
& - \left(\frac{\eta^n - \eta^{n-1}}{\Delta t}, \phi_h^n \right) - v_f \left(\frac{\partial}{\partial x} \phi_h^n, \phi_h^n \right) - v_f \left(\frac{\partial}{\partial x} \eta^n, \phi_h^n \right) \\
& + \frac{2v_f}{\rho_m} (b(\eta^n, \rho^n, \phi_h^n) + b(\phi_h^n, \rho^n, \phi_h^n) + b(\rho_h^n, \eta^n, \phi_h^n)) - \chi\delta^2 \left(\frac{\partial}{\partial x} \eta^{n*}, \frac{\partial}{\partial x} \phi_h^{n*} \right) \\
& + \left(\frac{\rho^n - \rho^{n-1}}{\Delta t} - \frac{\partial}{\partial t} \rho^n, \phi_h^n \right) + \chi\delta^2 \left(\frac{\partial}{\partial x} \rho^{n*}, \frac{\partial}{\partial x} \phi_h^{n*} \right) \\
& \leq |T_0| + |T_1| + |T_2| + |T_3| + |T_4| + |T_5| + |T_6| + |T_7| + |T_8|. \tag{22}
\end{aligned}$$

Now we bound each T_i term individually. T_0 is bounded as

$$\begin{aligned}
|T_0| & \leq \frac{1}{4} \left\| \frac{\eta^n - \eta^{n-1}}{\Delta t} \right\|^2 + \|\phi_h^n\|^2 \\
& \leq \frac{1}{4} \int_{\Omega} \left(\frac{1}{\Delta t} \int_{t^{n-1}}^{t^n} |\eta_t| dt \right)^2 dx + \|\phi_h^n\|^2 \\
& \leq \frac{1}{4\Delta t} \int_{t^{n-1}}^{t^n} \|\eta_t\|^2 dt + \|\phi_h^n\|^2. \tag{23}
\end{aligned}$$

T_1 vanishes by periodicity of $\phi_h^n \in X_h$ and the fundamental theorem of Calculus

$$|T_1| = v_f \left| \left(\frac{\partial}{\partial x} \phi_h^n, \phi_h^n \right) \right| = v_f \left| \int_{\Omega} \frac{\partial \phi_h^n}{\partial x} \phi_h^n dx \right| \leq v_f \int_{\Omega} \frac{1}{2} \frac{\partial}{\partial x} |\phi_h^n|^2 dx = 0. \tag{24}$$

Using integration by parts and $\phi_h = \phi_h^* + D_N^h \overline{\phi_h^n}^h$ along with Lemma 2.1 we have

$$\begin{aligned}
|T_2| & \leq v_f \left| \left(\eta^n, \frac{\partial}{\partial x} \phi_h^n \right) \right| \leq v_f \left| \left(\eta^n, \frac{\partial}{\partial x} \phi_h^{n*} \right) \right| + v_f \left| \left(\eta^n, \frac{\partial}{\partial x} D_N^h \overline{\phi_h^n}^h \right) \right| \\
& \leq \frac{Cv_f^2}{\chi\delta^2} \|\eta^n\|^2 + \frac{\chi\delta^2}{12} \left\| \frac{\partial}{\partial x} \phi_h^{n*} \right\|^2 + v_f \|\eta^n\| \left\| \frac{\partial}{\partial x} D_N^h \overline{\phi_h^n}^h \right\| \\
& \leq \frac{Cv_f^2}{\chi\delta^2} \|\eta^n\|^2 + \frac{\chi\delta^2}{12} \left\| \frac{\partial}{\partial x} \phi_h^{n*} \right\|^2 + v_f^2 \frac{C^2(N)}{\delta^2} \|\eta^n\|^2 + \frac{1}{4} \|\phi_h^n\|^2. \tag{25}
\end{aligned}$$

To bound $|T_3|$ we use Lemma 2.5 equation (6)

$$|T_3| = \frac{2v_f}{\rho_m} |b(\eta^n, \rho^n, \phi_h^n)| = \frac{2v_f}{3\rho_m} \left| \int_{\Omega} \eta^n \frac{\partial \rho^n}{\partial x} \phi_h^n dx - \int_{\Omega} \eta^n \frac{\partial \phi_h^n}{\partial x} \rho^n dx \right|. \quad (26)$$

The first term in (26) is bounded as

$$\begin{aligned} \left| \int_{\Omega} \eta^n \frac{\partial \rho^n}{\partial x} \phi_h^n dx \right| &\leq \int_{\Omega} \left| \eta^n \frac{\partial \rho^n}{\partial x} \phi_h^n \right| dx \\ &\leq \|\eta^n\| \|\phi_h^n\| \left\| \frac{\partial \rho^n}{\partial x} \right\|_{L^\infty} \leq C \|\eta^n\| \|\phi_h^n\|, \end{aligned}$$

and the second term in (26) is bounded as

$$\begin{aligned} \left| \int_{\Omega} \eta^n \frac{\partial \phi_h^n}{\partial x} \rho^n dx \right| &\leq \|\eta^n\| \left\| \frac{\partial \phi_h^n}{\partial x} \right\| \|\rho^n\|_{L^\infty} \leq C \|\eta^n\| \left\| \frac{\partial \phi_h^n}{\partial x} \right\| \\ &\leq C \|\eta^n\| \left(\left\| \frac{\partial}{\partial x} \phi_h^{n*} \right\| + \left\| \frac{\partial}{\partial x} D_N^h \overline{\phi_h^{n*}} \right\| \right). \end{aligned}$$

Therefore, by triangle inequality we have that $|T_3|$ has the bound

$$|T_3| \leq C \frac{2v_f}{3\rho_m} \left(\|\phi_h^n\| + \left\| \frac{\partial}{\partial x} \phi_h^{n*} \right\| + \left\| \frac{\partial}{\partial x} D_N^h \overline{\phi_h^{n*}} \right\| \right) \|\eta^n\|. \quad (27)$$

To bound $|T_4|$ we use formulas (8),(9) to get

$$\begin{aligned} |T_4| &= \frac{2v_f}{\rho_m} |b(\phi_h^n, \rho^n, \phi_h^n)| = \frac{2v_f}{\rho_m} \left| \frac{2}{3} \int_{\Omega} \phi_h^n \frac{\partial \rho^n}{\partial x} \phi_h^n dx + \frac{1}{3} \int_{\Omega} \rho^n \frac{\partial \phi_h^n}{\partial x} \phi_h^n dx \right| \\ &\leq \frac{v_f}{\rho_m} \int_{\Omega} \left| \phi_h^n \frac{\partial \rho^n}{\partial x} \phi_h^n \right| dx \leq \frac{v_f}{\rho_m} \left\| \frac{\partial \rho^n}{\partial x} \right\|_{L^\infty} \|\phi_h^n\|^2 \leq \frac{v_f}{\rho_m} C \|\phi_h^n\|^2. \end{aligned} \quad (28)$$

Using $\rho_h^n = I_h^n - \phi_h^n$ we obtain

$$|T_5| = \frac{2v_f}{\rho_m} |b(\rho_h^n, \eta^n, \phi_h^n)| = \frac{2v_f}{\rho_m} |b(I_h^n, \eta^n, \phi_h^n) - b(\phi_h^n, \eta^n, \phi_h^n)|. \quad (29)$$

We estimate each term on the right hand side of (29) separately. Starting

with the first term, we can use formula (7) and bound similarly to $|T_3|$

$$\begin{aligned}
|b(I_h^n, \eta^n, \phi_h^n)| &\leq \frac{1}{3} \int_{\Omega} \left| \eta^n \frac{\partial I_h^n}{\partial x} \phi_h^n \right| dx + \frac{2}{3} \int_{\Omega} \left| \eta^n \frac{\partial \phi_h^n}{\partial x} I_h^n \right| dx \\
&\leq \frac{1}{3} \|\eta^n\| \|\phi_h^n\| \left\| \frac{\partial}{\partial x} I_h^n \right\|_{L^\infty} + \frac{2}{3} \|\eta^n\| \left\| \frac{\partial}{\partial x} \phi_h^n \right\| \|I_h^n\|_{L^\infty} \\
&\leq C \left(\|\phi_h^n\| + \left\| \frac{\partial}{\partial x} \phi_h^{n*} \right\| + \left\| \frac{\partial}{\partial x} D_N^h \overline{\phi_h^{n*}} \right\| \right) \|\eta^n\|. \quad (30)
\end{aligned}$$

Following the same approach as in $|T_4|$, the second term is bounded as

$$\frac{2v_f}{\rho_m} |b(\phi_h^n, \eta^n, \phi_h^n)| \leq \frac{v_f}{\rho_m} \left\| \frac{\partial}{\partial x} \eta^n \right\|_{L^\infty} \|\phi_h^n\|^2 \leq \frac{v_f}{\rho_m} C \|\phi_h^n\|^2. \quad (31)$$

Combining (30) and (31) yields

$$|T_5| \leq C \frac{2v_f}{\rho_m} \left(\|\phi_h^n\| + \left\| \frac{\partial}{\partial x} \phi_h^{n*} \right\| + \left\| \frac{\partial}{\partial x} D_N^h \overline{\phi_h^{n*}} \right\| \right) \|\eta^n\| + \frac{v_f}{\rho_m} C \|\phi_h^n\|^2. \quad (32)$$

To bound $|T_6|$ we simply apply the Cauchy-Schwarz inequality followed by Young's inequality

$$|T_6| \leq \chi \delta^2 \left\| \frac{\partial}{\partial x} \eta^{n*} \right\| \left\| \frac{\partial}{\partial x} \phi_h^{n*} \right\| \leq 3\chi \delta^2 \left\| \frac{\partial}{\partial x} \eta^{n*} \right\|^2 + \frac{\chi \delta^2}{12} \left\| \frac{\partial}{\partial x} \phi_h^{n*} \right\|^2. \quad (33)$$

$|T_7|$ is bounded with Cauchy-Schwarz and Young's inequalities, and an application of Taylor's remainder formula resulting in

$$\begin{aligned}
|T_7| &\leq \frac{1}{4} \|\phi_h^n\|^2 + \left\| \rho_t^n - \frac{1}{\Delta t} (\rho^n - \rho^{n-1}) \right\|^2 \\
&\leq \frac{1}{4} \|\phi_h^n\|^2 + C \Delta t \int_{t^{n-1}}^{t^n} \|\rho_{tt}\|^2 dt. \quad (34)
\end{aligned}$$

Lastly, $|T_8|$ is bounded as

$$|T_8| \leq \chi \delta^2 \left\| \frac{\partial}{\partial x} \rho^{n*} \right\| \left\| \frac{\partial}{\partial x} \phi_h^{n*} \right\| \leq 3\chi \delta^2 \left\| \frac{\partial}{\partial x} \rho^{n*} \right\|^2 + \frac{\chi \delta^2}{12} \left\| \frac{\partial}{\partial x} \phi_h^{n*} \right\|^2. \quad (35)$$

Applying the bounds (23) - (35) to (22) and simplifying results in

$$\begin{aligned}
& \frac{1}{2\Delta t} \left(\|\phi_h^n\|^2 - \|\phi_h^{n-1}\|^2 \right) + \frac{3\chi\delta^2}{4} \left\| \frac{\partial}{\partial x} \phi_h^{n*} \right\|^2 \leq 3\chi\delta^2 \left(\left\| \frac{\partial}{\partial x} \rho^{n*} \right\|^2 + \left\| \frac{\partial}{\partial x} \eta^{n*} \right\|^2 \right) \\
+ & \quad C \frac{v_f^2}{\delta^2} \left(\frac{1}{\chi} + 1 \right) \|\eta^n\|^2 + \left(C \frac{v_f}{\rho_m} + \frac{3}{2} \right) \|\phi_h^n\|^2 + C\Delta t \int_{t^{n-1}}^{t^n} \|\rho_{tt}\|^2 dt \\
+ & \quad C \frac{v_f}{\rho_m} \left(\|\phi_h^n\| + \left\| \frac{\partial}{\partial x} \phi_h^{n*} \right\| + \left\| \frac{\partial}{\partial x} D_N^h \overline{\phi_h^{n*}} \right\| \right) \|\eta^n\| + \frac{1}{4\Delta t} \int_{t^{n-1}}^{t^n} \|\eta_t\|^2 dt. \tag{36}
\end{aligned}$$

We further bound the last terms in (36) using Young's inequality and Lemma 2.1 giving

$$\begin{aligned}
& C \frac{v_f}{\rho_m} \left(\|\phi_h^n\| + \left\| \frac{\partial}{\partial x} \phi_h^{n*} \right\| + \left\| \frac{\partial}{\partial x} D_N^h \overline{\phi_h^{n*}} \right\| \right) \|\eta^n\| \\
\leq & \quad \frac{1}{4} \|\phi_h^n\|^2 + \frac{Cv_f^2}{\rho_m^2} \|\eta^n\|^2 + \frac{\chi\delta^2}{4} \left\| \frac{\partial}{\partial x} \phi_h^{n*} \right\|^2 + \\
& \frac{Cv_f^2}{\rho_m^2 \chi \delta^2} \|\eta^n\|^2 + \frac{1}{4} \|\phi_h^n\|^2 + \frac{Cv_f^2}{\rho_m^2 \delta^2} \|\eta^n\|^2. \tag{37}
\end{aligned}$$

Plugging in (37) into (36) yields

$$\begin{aligned}
& \frac{1}{2\Delta t} \left(\|\phi_h^n\|^2 - \|\phi_h^{n-1}\|^2 \right) + \frac{\chi\delta^2}{2} \left\| \frac{\partial}{\partial x} \phi_h^{n*} \right\|^2 \leq 3\chi\delta^2 \left(\left\| \frac{\partial}{\partial x} \rho^{n*} \right\|^2 + \left\| \frac{\partial}{\partial x} \eta^{n*} \right\|^2 \right) \\
+ & \quad C \frac{v_f^2}{\delta^2} \left(\frac{1}{\chi} + 1 \right) \|\eta^n\|^2 + \left(C \frac{v_f}{\rho_m} + 2 \right) \|\phi_h^n\|^2 + C\Delta t \int_{t^{n-1}}^{t^n} \|\rho_{tt}\|^2 dt \\
+ & \quad C \frac{v_f^2}{\rho_m^2} \left(1 + \frac{1}{\chi\delta^2} + \frac{1}{\delta^2} \right) \|\eta^n\|^2 + \frac{1}{4\Delta t} \int_{t^{n-1}}^{t^n} \|\eta_t\|^2 dt. \tag{38}
\end{aligned}$$

Multiplying by $2\Delta t$, summing up from $n = 1$ to M , and recalling that $\|\phi_h^0\| =$

0 gives

$$\begin{aligned}
& \|\phi_h^M\|^2 + \chi\delta^2\Delta t \sum_{n=1}^M \left\| \frac{\partial}{\partial x} \phi_h^{n*} \right\|^2 \\
& \leq 6\chi\delta^2\Delta t \sum_{n=1}^M \left(\left\| \frac{\partial}{\partial x} \rho^{n*} \right\|^2 + \left\| \frac{\partial}{\partial x} \eta^{n*} \right\|^2 \right) + C \frac{v_f^2}{\delta^2} \left(\frac{1}{\chi} + 1 \right) \Delta t \sum_{n=1}^M \|\eta^n\|^2 \\
& \quad + \left(C \frac{v_f}{\rho_m} + 2 \right) \Delta t \sum_{n=1}^M \|\phi_h^n\|^2 + C\Delta t^2 \int_{t^0}^{t^M} \|\rho_{tt}\|^2 dt \\
& \quad + C \frac{v_f^2}{\rho_m^2} \left(1 + \frac{1}{\chi\delta^2} + \frac{1}{\delta^2} \right) \Delta t \sum_{n=1}^M \|\eta^n\|^2 + \frac{1}{2} \int_{t^0}^{t^M} \|\eta_t\|^2 dt. \tag{39}
\end{aligned}$$

Using the standard interpolation inequalities (2), (3) and Lemma 2.2, we have

$$\begin{aligned}
& \|\phi_h^M\|^2 + \chi\delta^2 \left\| \left\| \frac{\partial}{\partial x} \phi_h^{n*} \right\| \right\|_{2,0}^2 \leq \chi\delta^{4N+6} \left\| \left\| \frac{\partial \rho}{\partial x} \right\| \right\|_{2,2N+3}^2 \\
& + C(N)\chi(\delta^2 h^{2k} + h^{2k+2}) \|\rho\|_{2,k+1}^2 \\
& + 6\chi\delta^2 h^{2k} \|\rho\|_{2,k+1}^2 + C \frac{v_f^2}{\delta^2} \left(\frac{1}{\chi} + 1 \right) h^{2k+2} \|\rho\|_{2,k+1}^2 \\
& + C \left(\frac{v_f}{\rho_m} + 1 \right) \Delta t \sum_{n=1}^M \|\phi_h^n\|^2 + C\Delta t^2 \int_{t^0}^{t^M} \|\rho_{tt}\|^2 dt \\
& + C \frac{v_f^2}{\rho_m^2} \left(1 + \frac{1}{\chi\delta^2} + \frac{1}{\delta^2} \right) h^{2k+2} \|\rho\|_{2,k+1}^2 + Ch^{2k+2} \int_{t^0}^{t^M} \|\rho_t\|_{k+1}^2 dt.
\end{aligned}$$

Thus, with a sufficiently small time step ($\gamma_n \Delta t := C(\frac{v_f}{\rho_m} + 1)\Delta t \leq 1$), applying the Gronwall inequality from Lemma 2.4 results in

$$\begin{aligned}
& \|\phi_h^M\|^2 + \chi\delta^2 \left\| \left\| \frac{\partial}{\partial x} \phi_h^{n*} \right\| \right\|_{2,0}^2 \leq C \exp \left(\Delta t \sum_{n=0}^M \frac{\gamma}{1 - \Delta t \gamma_n} \right) \left(\chi\delta^{4N+6} \left\| \left\| \frac{\partial \rho}{\partial x} \right\| \right\|_{2,2N+3}^2 \right. \\
& + \chi h^{2k+2} \|\rho\|_{2,k+1}^2 + \chi\delta^2 h^{2k} \|\rho\|_{2,k+1}^2 \\
& + \frac{v_f^2}{\delta^2} \left(\frac{1}{\chi} + 1 \right) h^{2k+2} \|\rho\|_{2,k+1}^2 + h^{2k+2} \int_{t^0}^{t^M} \|\rho_t\|_{k+1}^2 dt \\
& \left. + \Delta t^2 \int_{t^0}^{t^M} \|\rho_{tt}\|^2 dt + \frac{v_f^2}{\rho_m^2} \left(1 + \frac{1}{\chi\delta^2} + \frac{1}{\delta^2} \right) h^{2k+2} \|\rho\|_{2,k+1}^2 \right).
\end{aligned}$$

Employing triangle inequality completes the proof. \square

Remark 3.1. For a smooth solution ρ and dropping higher order terms, the above error estimate becomes

$$\|\rho - \rho_h\|_{\infty,0}^2 = O(\Delta t^2 + \chi \delta^{4N+6} + \chi \delta^2 h^{2k} + \chi^{-1} \delta^{-2} h^{2k+2} + \delta^{-2} h^{2k+2}).$$

Hence, to obtain the highest rates we choose $\delta = h^{0.5}$, i.e.,

$$\|\rho - \rho_h\|_{\infty,0}^2 = O(\Delta t^2 + \chi h^{2N+3} + (\chi + \chi^{-1} + 1)h^{2k+1}).$$

Next we will prove the convergence analysis for solutions of Algorithm 2.2.

Theorem 3.2. Let ρ_h^n be the solution of Algorithm 2.2 given by (17) and ρ be a solution of (1) with enough regularity. Then, for sufficiently small Δt we have

$$\begin{aligned} & \frac{1}{4} \left(\|e^M\|^2 + \|2e^M - e^{M-1}\|^2 + \|e^M - e^{M-1}\|^2 \right) \\ & + \frac{3}{4} \sum_{n=2}^M \|e^n - e^{n-1} - e^{n-2}\|^2 \leq CK \left(h^{2k+2} \|\rho\|_{\infty,k+1}^2 \right. \\ & + \chi(\delta^2 h^{2k} + h^{2k+2}) \|\rho\|_{2,k+1}^2 + \chi \delta^{4N+6} \left\| \left\| \frac{\partial \rho}{\partial x} \right\| \right\|_{2,2N+3}^2 \\ & + \chi \delta^2 h^{2k} \|\rho\|_{2,k+1}^2 + \frac{v_f^2}{\delta^2} \left(\frac{1}{\chi} + 1 \right) h^{2k+2} \|\rho\|_{2,k+1}^2 \\ & + \frac{v_f^2}{\rho_m^2} \left(1 + \frac{1}{\chi \delta^2} + \frac{1}{\delta^2} \right) h^{2k+2} \|\rho\|_{2,k+1}^2 + \Delta t^4 \int_{t^0}^{t^M} \|\rho_{ttt}\|^2 dt \\ & + \left(v_f^2 + \frac{v_f}{\rho_m} \right) \Delta t^4 \int_{t^0}^{t^M} \left\| \frac{\partial}{\partial x} \rho_{tt} \right\|^2 dt + \frac{v_f}{\rho_m} \Delta t^4 \int_{t^0}^{t^M} \|\rho_{tt}\|^2 dt \Big). \end{aligned}$$

where $e^n = \rho^n - \rho_h^n$, and $K = \exp \left(\Delta t \sum_{n=0}^M \frac{\gamma_n}{1 - \Delta t \gamma_n} \right)$ and $\gamma_n = C \left(\frac{v_f}{\rho_m} + 1 \right)$.

Proof. Evaluating the weak formulation of (1) at time t^n yields

$$\begin{aligned} & \frac{1}{\Delta t} (D[\rho^n], v_h) + v_f \left(\frac{\partial}{\partial x} I[\rho^n], v_h \right) - \frac{2v_f}{\rho_m} b(I[\rho^n], I[\rho^n], v_h) \\ & + \chi \delta^2 \left(\frac{\partial}{\partial x} I[\rho^n]^*, \frac{\partial}{\partial x} v_h^* \right) = \tau(\rho^n, v_h), \end{aligned} \quad (40)$$

where the consistency error, τ , is given by

$$\begin{aligned} \tau(\rho^n, v_h) &:= \left(\frac{D[\rho^n]}{\Delta t} - \rho_t^n, v_h \right) + v_f \left(\frac{\partial}{\partial x} (I[\rho^n] - \rho^n), v_h \right) \\ &+ \frac{2v_f}{\rho_m} (b(\rho^n, \rho^n, v_h) - b(I[\rho^n], I[\rho^n], v_h)) + \chi \delta^2 \left(\frac{\partial}{\partial x} I[\rho^n]^*, \frac{\partial}{\partial x} v_h^* \right). \end{aligned}$$

Subtracting (17) from (40) gives the error equation,

$$\begin{aligned} &\frac{1}{\Delta t} (D[e^n], v_h) + v_f \left(\frac{\partial}{\partial x} I[e^n], v_h \right) - \frac{2v_f}{\rho_m} b(I[e^n], I[\rho^n], v_h) \\ &- \frac{2v_f}{\rho_m} b(I[\rho_h^n], I[e^n], v_h) + \chi \delta^2 \left(\frac{\partial}{\partial x} I[e^n]^*, \frac{\partial}{\partial x} v_h^* \right) = \tau(\rho^n, v_h). \end{aligned} \quad (41)$$

We again decompose the error as $e^n = \rho^n - I_h^n + I_h^n - \rho_h^n = \eta^n + \phi_h^n$ and pick $v_h = I[\phi_h^n]$ so that (41) becomes

$$\begin{aligned} &\frac{1}{\Delta t} (D[\phi_h^n], I[\phi_h^n]) + \chi \delta^2 \left\| \frac{\partial}{\partial x} I[\phi_h^n]^* \right\|^2 = -\frac{1}{\Delta t} (D[\eta^n], I[\phi_h^n]) \\ &- v_f \left(\frac{\partial}{\partial x} I[\phi_h^n], I[\phi_h^n] \right) - v_f \left(\frac{\partial}{\partial x} I[\eta^n], I[\phi_h^n] \right) \\ &+ \frac{2v_f}{\rho_m} (b(I[\eta^n], I[\rho^n], I[\phi_h^n]) + b(I[\phi_h^n], I[\rho^n], I[\phi_h^n]) + b(I[\rho_h^n], I[\eta^n], I[\phi_h^n])) \\ &- \chi \delta^2 \left(\frac{\partial}{\partial x} I[\eta^n]^*, \frac{\partial}{\partial x} I[\phi_h^n]^* \right) + \tau(\rho^n, I[\phi_h^n]) \end{aligned} \quad (42)$$

We now bound the first and last terms on the right-hand side, while the rest of them are handled similarly to the ones in Theorem 3.1.

Using Lemma 2.3 for the first term, we have

$$(D[\phi_h^n], I[\phi_h^n]) = \mathcal{E}[\phi_h^n] - \mathcal{E}[\phi_h^{n-1}] + \mathcal{Z}[\phi_h^n].$$

For the last term, the consistency error $\tau(\rho^n, I[\phi_h^n])$, we have the following bounds

$$\begin{aligned} \left(\frac{D[\rho^n]}{\Delta t} - \rho_t^n, I[\phi_h^n] \right) &\leq \frac{1}{4\epsilon} \left\| \frac{D[\rho^n]}{\Delta t} - \rho_t^n \right\|^2 + \epsilon \|I[\phi_h^n]\|^2 \\ &\leq \frac{1}{4\epsilon} \frac{6}{5} \Delta t^3 \int_{t^{n-2}}^{t^n} \|\rho_{ttt}\|^2 dt + \epsilon \|I[\phi_h^n]\|^2, \end{aligned}$$

$$\begin{aligned}
v_f \left(\frac{\partial}{\partial x} (I[\rho^n] - \rho^n), I[\phi_h^n] \right) &\leq v_f^2 \frac{1}{4\varepsilon} \left\| \frac{\partial}{\partial x} (I[\rho^n] - \rho^n) \right\|^2 + \varepsilon \|I[\phi_h^n]\|^2 \\
&\leq \frac{v_f^2}{3\varepsilon} \Delta t^3 \int_{t^{n-2}}^{t^n} \left\| \frac{\partial}{\partial x} \rho_{tt} \right\|^2 dt + \varepsilon \|I[\phi_h^n]\|^2.
\end{aligned}$$

The trilinear terms are bounded similarly to T_4

$$\begin{aligned}
&b(\rho^n, \rho^n, I[\phi_h^n]) - b(I[\rho^n], I[\rho^n], I[\phi_h^n]) \\
&= b(\rho^n - I[\rho^n], \rho^n, I[\phi_h^n]) - b(I[\rho^n], \rho^n - I[\rho^n], I[\phi_h^n]) \\
&\leq \|\rho^n - I[\rho^n]\| \left\| \frac{\partial}{\partial x} \rho^n \right\|_{L^\infty} \|I[\phi_h^n]\| + \|I[\rho^n]\|_{L^\infty} \left\| \frac{\partial}{\partial x} (\rho^n - I[\rho^n]) \right\| \|I[\phi_h^n]\| \\
&\leq \|\rho^n - I[\rho^n]\| C \|I[\phi_h^n]\| + C \left\| \frac{\partial}{\partial x} (\rho^n - I[\rho^n]) \right\| \|I[\phi_h^n]\| \\
&\leq \frac{C}{\varepsilon} \|\rho^n - I[\rho^n]\|^2 + \frac{C}{\varepsilon} \left\| \frac{\partial}{\partial x} (\rho^n - I[\rho^n]) \right\|^2 + \varepsilon \|I[\phi_h^n]\|^2 \\
&\leq \frac{C}{\varepsilon} \Delta t^3 \int_{t^{n-2}}^{t^n} \|\rho_{tt}\|^2 dt + \frac{C}{\varepsilon} \Delta t^3 \int_{t^{n-2}}^{t^n} \left\| \frac{\partial}{\partial x} \rho_{tt} \right\|^2 dt + \varepsilon \|I[\phi_h^n]\|^2,
\end{aligned}$$

$$\begin{aligned}
\chi \delta^2 \left(\frac{\partial}{\partial x} I[\rho^n]^*, \frac{\partial}{\partial x} I[\phi_h^n]^* \right) &\leq \chi \delta^2 \left\| \frac{\partial}{\partial x} I[\rho^n]^* \right\| \left\| \frac{\partial}{\partial x} I[\phi_h^n]^* \right\| \\
&\leq \frac{\chi \delta^2}{4\varepsilon} \left\| \frac{\partial}{\partial x} I[\rho^n]^* \right\|^2 + \varepsilon \chi \delta^2 \left\| \frac{\partial}{\partial x} I[\phi_h^n]^* \right\|^2.
\end{aligned}$$

Combining all the previous bounds into (42) and setting $\varepsilon = \frac{1}{3}$ gives

$$\begin{aligned}
&\frac{1}{\Delta t} (\mathcal{E}[\phi_h^n] - \mathcal{E}[\phi_h^{n-1}] + \mathcal{Z}[\phi_h^n]) + \frac{\chi \delta^2}{4} \left\| \frac{\partial}{\partial x} I[\phi_h^n]^* \right\|^2 \leq \\
&C \chi \delta^2 \left(\left\| \frac{\partial}{\partial x} I[\rho^n]^* \right\|^2 + \left\| \frac{\partial}{\partial x} I[\eta^n]^* \right\|^2 \right) + \frac{C v_f^2}{\delta^2} \left(\frac{1}{\chi} + 1 \right) \|I[\eta^n]\|^2 \\
&\quad + \frac{C v_f^2}{\rho_m^2} \left(1 + \frac{1}{\chi \delta^2} + \frac{1}{\delta^2} \right) \|I[\eta^n]\|^2 + C \left(\frac{v_f}{\rho_m} + 1 \right) \|I[\phi_h^n]\|^2 \\
&\quad + C \Delta t^3 \int_{t^{n-2}}^{t^n} \|\rho_{ttt}\|^2 dt + C \left(v_f^2 + \frac{v_f}{\rho_m} \right) \Delta t^3 \int_{t^{n-2}}^{t^n} \left\| \frac{\partial}{\partial x} \rho_{tt} \right\|^2 dt \\
&\quad \quad \quad + \frac{C v_f}{\rho_m} \Delta t^3 \int_{t^{n-2}}^{t^n} \|\rho_{tt}\|^2 dt.
\end{aligned}$$

Multiplying by $4\Delta t$ and summing from $n = 2, \dots, M$ yields

$$\begin{aligned}
& 4(\mathcal{E}[\phi^M] - \mathcal{E}[\phi^1]) + 4\Delta t \sum_{n=2}^M \mathcal{Z}[\phi^n] + \chi \delta^2 \Delta t \sum_{n=2}^M \left\| \frac{\partial}{\partial x} I[\phi_h^n]^* \right\|^2 \leq \\
& C\chi \delta^2 \Delta t \sum_{n=2}^M \left(\left\| \frac{\partial}{\partial x} I[\rho^n]^* \right\|^2 + \left\| \frac{\partial}{\partial x} I[\eta^n]^* \right\|^2 \right) + \frac{Cv_f^2}{\delta^2} \left(\frac{1}{\chi} + 1 \right) \Delta t \sum_{n=2}^M \|I[\eta^n]\|^2 \\
& \quad + \frac{Cv_f^2}{\rho_m^2} \left(1 + \frac{1}{\chi \delta^2} + \frac{1}{\delta^2} \right) \Delta t \sum_{n=2}^M \|I[\eta^n]\|^2 \\
& \quad + C \left(\frac{v_f}{\rho_m} + 1 \right) \Delta t \sum_{n=2}^M \|I[\phi_h^n]\|^2 + C\Delta t^4 \int_{t^0}^{t^M} \|\rho_{ttt}\|^2 dt \\
& \quad + C \left(v_f^2 + \frac{v_f}{\rho_m} \right) \Delta t^4 \int_{t^0}^{t^M} \left\| \frac{\partial}{\partial x} \rho_{tt} \right\|^2 dt + \frac{Cv_f}{\rho_m} \Delta t^4 \int_{t^0}^{t^M} \|\rho_{tt}\|^2 dt.
\end{aligned}$$

Applying the standard interpolation inequalities (2), (3), and Lemma 2.2, we have

$$\begin{aligned}
& 4(\mathcal{E}[\phi^M] - \mathcal{E}[\phi^1]) + 4\Delta t \sum_{n=2}^M \mathcal{Z}[\phi^n] + \chi \delta^2 \Delta t \sum_{n=2}^M \left\| \frac{\partial}{\partial x} I[\phi_h^n]^* \right\|^2 \leq \\
& + C(N)\chi(\delta^2 h^{2k} + h^{2k+2}) \|\rho\|_{2,k+1}^2 + \chi \delta^{4N+6} \left\| \left\| \frac{\partial \rho}{\partial x} \right\| \right\|_{2,2N+3}^2 + C\chi \delta^2 h^{2k} \|\rho\|_{2,k+1}^2 \\
& + \frac{Cv_f^2}{\delta^2} \left(\frac{1}{\chi} + 1 \right) h^{2k+2} \|\rho\|_{2,k+1}^2 + \frac{Cv_f^2}{\rho_m^2} \left(1 + \frac{1}{\chi \delta^2} + \frac{1}{\delta^2} \right) h^{2k+2} \|\rho\|_{2,k+1}^2 \\
& \quad + C \left(\frac{v_f}{\rho_m} + 1 \right) \Delta t \sum_{n=2}^M \|I[\phi_h^n]\|^2 + C\Delta t^4 \int_{t^0}^{t^M} \|\rho_{ttt}\|^2 dt \\
& \quad + C \left(v_f^2 + \frac{v_f}{\rho_m} \right) \Delta t^4 \int_{t^0}^{t^M} \left\| \frac{\partial}{\partial x} \rho_{tt} \right\|^2 dt + \frac{Cv_f}{\rho_m} \Delta t^4 \int_{t^0}^{t^M} \|\rho_{tt}\|^2 dt.
\end{aligned}$$

Thus, applying the Gronwall inequality from Lemma 2.4 with a suffi-

ciently small time step ($\gamma_n \Delta t := C(\frac{v_f}{\rho_m} + 1)\Delta t \leq 1$), we obtain

$$\begin{aligned}
& 4\mathcal{E}[\phi^M] + 4\Delta t \sum_{n=2}^M \mathcal{Z}[\phi^n] + \chi \delta^2 \Delta t \sum_{n=2}^M \left\| \frac{\partial}{\partial x} I[\phi_h^n]^* \right\|^2 \leq \\
& + CK \left(\mathcal{E}[\phi^1] + \chi(\delta^2 h^{2k} + h^{2k+2}) \|\rho\|_{2,k+1}^2 + \chi \delta^{4N+6} \left\| \frac{\partial \rho}{\partial x} \right\|_{2,2N+3}^2 \right. \\
& \quad + \chi \delta^2 h^{2k} \|\rho\|_{2,k+1}^2 + \frac{v_f^2}{\delta^2} \left(\frac{1}{\chi} + 1 \right) h^{2k+2} \|\rho\|_{2,k+1}^2 \\
& \quad + \frac{v_f^2}{\rho_m^2} \left(1 + \frac{1}{\chi \delta^2} + \frac{1}{\delta^2} \right) h^{2k+2} \|\rho\|_{2,k+1}^2 + \Delta t^4 \int_{t^0}^{t^M} \|\rho_{ttt}\|^2 dt \\
& \quad \left. + \left(v_f^2 + \frac{v_f}{\rho_m} \right) \Delta t^4 \int_{t^0}^{t^M} \left\| \frac{\partial}{\partial x} \rho_{tt} \right\|^2 dt + \frac{v_f}{\rho_m} \Delta t^4 \int_{t^0}^{t^M} \|\rho_{tt}\|^2 dt \right),
\end{aligned}$$

where $K = \exp \left(\Delta t \sum_{n=0}^M \frac{\gamma_n}{1 - \Delta t \gamma_n} \right)$. Note that $\mathcal{E}[\phi^1]$ is bounded as in [8], i.e.,

$$\mathcal{E}[\phi^1] \leq C \left(\|\rho^1 - \rho_h^1\|^2 + \|\rho^0 - \rho_h^0\|^2 \right) + Ch^{2k+2} \|\rho\|_{\infty,k+1}^2,$$

where the error in the first time step is bounded by employing Theorem 3.1 with $M = 1$. Applying triangle inequality and substituting 15 and 16 completes the proof. \square

Remark 3.2. For a smooth solution ρ , after dropping higher order terms and again picking $\delta = h^{0.5}$, the error estimate transforms into

$$\|\rho - \rho_h\|_{\infty,0}^2 = O \left(\Delta t^4 + \chi h^{2N+3} + (\chi + \chi^{-1} + 1) h^{2k+1} \right).$$

4. Computational Experiments

4.1. Convergence Rate Simulations

We now turn our attention to verifying the results of Theorem 3.1 on the 1D domain $[0, 1]$. We employ the manufactured solution $\rho(x, t) = \sin^4(\pi x) \sin(t)$ to the Dirichlet problem

$$\begin{cases} \frac{\partial \rho}{\partial t} + \left(v_f - \frac{2v_f}{\rho_m} \rho \right) \frac{\partial \rho}{\partial x} = f, & x \in (0, 1), t > 0, \\ \rho(0, t) = \rho(1, t) = 0, & x \in \{0, 1\}, t > 0, \\ \rho(x, 0) = 0, & x \in [0, 1], t = 0, \end{cases}$$

where $v_f = \rho_m = 1$, and

$$f(x, t) = \sin^4(\pi x) \cos(t) + 4\pi \cos(\pi x) \sin^3(\pi x) \sin(t) \left(v_f - \frac{2v_f}{\rho_m} \sin^4(\pi x) \sin(t) \right).$$

Based on Remark 3.1, we observe the spatial rate of convergence, in the $P2$ finite element space with order of deconvolution $N = 1$, to be $\mathcal{O}(h^{2.5})$ with stabilization and $\mathcal{O}(h^2)$ without stabilization. Tables 1-2 exhibit these rates for a simulation where final time $T = 0.02$, $\Delta t = 5 \times 10^{-6}$, and $\delta = 0.1\sqrt{h}$.

h	No time filter ($\gamma = 0$)		Time filter ($\gamma = \frac{2}{3}$)	
	$\ \rho - \rho_h\ _{\ell^\infty(0,T;L^2)}$	Rate	$\ \rho - \rho_h\ _{\ell^\infty(0,T;L^2)}$	Rate
$\frac{1}{6}$	9.58×10^{-5}	—	9.28×10^{-5}	—
$\frac{1}{12}$	1.46×10^{-5}	2.71	1.34×10^{-5}	2.79
$\frac{1}{24}$	2.67×10^{-6}	2.45	2.68×10^{-6}	2.32
$\frac{1}{48}$	6.23×10^{-7}	2.10	6.26×10^{-7}	2.10
$\frac{1}{96}$	1.55×10^{-7}	2.01	1.53×10^{-7}	2.03
$\frac{1}{192}$	3.84×10^{-8}	2.01	3.82×10^{-8}	2.00

Table 1: Space rates for $\chi = 0$

h	No time filter ($\gamma = 0$)		Time filter ($\gamma = \frac{2}{3}$)	
	$\ \rho - \rho_h\ _{\ell^\infty(0,T;L^2)}$	Rate	$\ \rho - \rho_h\ _{\ell^\infty(0,T;L^2)}$	Rate
$\frac{1}{6}$	8.78×10^{-5}	—	8.42×10^{-5}	—
$\frac{1}{12}$	1.35×10^{-5}	2.70	1.49×10^{-5}	2.50
$\frac{1}{24}$	2.54×10^{-6}	2.41	2.65×10^{-6}	2.49
$\frac{1}{48}$	5.51×10^{-7}	2.20	5.46×10^{-7}	2.28
$\frac{1}{96}$	1.12×10^{-7}	2.29	1.12×10^{-7}	2.28
$\frac{1}{192}$	2.10×10^{-8}	2.42	2.10×10^{-8}	2.42

Table 2: Space rates for $\chi = 1$

For the time convergence rate simulations, the finite element space is $P2$ and we set order of deconvolution $N = 1$, mesh size $h = \frac{1}{100}$, filter width $\delta = 0.1\sqrt{h}$, and final time $T = 1$.

Tables 3-4 display the expected time convergence rates without and with stabilization (i.e. $\chi = 0$ and $\chi = 1$ respectively), where the rate is 1 without time filtering, and 2 with time filtering. We observe that the stabilization makes little difference in both the errors and the rates.

Δt	No time filter ($\gamma = 0$)		Time filter ($\gamma = \frac{2}{3}$)	
	$\ \rho - \rho_h\ _{\ell^\infty(0,T;L^2)}$	Rate	$\ \rho - \rho_h\ _{\ell^\infty(0,T;L^2)}$	Rate
$\frac{1}{10}$	1.97×10^{-2}	—	4.88×10^{-3}	—
$\frac{1}{20}$	9.13×10^{-3}	1.11	1.26×10^{-3}	1.95
$\frac{1}{40}$	4.43×10^{-3}	1.04	3.29×10^{-4}	1.94
$\frac{1}{80}$	2.19×10^{-3}	1.02	8.48×10^{-5}	1.96
$\frac{1}{160}$	1.09×10^{-3}	1.01	2.31×10^{-5}	1.88

Table 3: Time rates for $\chi = 0$

Δt	No time filter ($\gamma = 0$)		Time filter ($\gamma = \frac{2}{3}$)	
	$\ \rho - \rho_h\ _{\ell^\infty(0,T;L^2)}$	Rate	$\ \rho - \rho_h\ _{\ell^\infty(0,T;L^2)}$	Rate
$\frac{1}{10}$	1.96×10^{-2}	—	4.87×10^{-3}	—
$\frac{1}{20}$	9.12×10^{-3}	1.10	1.26×10^{-3}	1.95
$\frac{1}{40}$	4.43×10^{-3}	1.04	3.29×10^{-4}	1.94
$\frac{1}{80}$	2.19×10^{-3}	1.02	8.43×10^{-5}	1.96
$\frac{1}{160}$	1.09×10^{-3}	1.01	2.15×10^{-5}	1.97

Table 4: Time rates for $\chi = 1$

4.2. Rarefaction

Here we examine the LWR model with the Greenshield's flow velocity relationship, with parameters $\rho_m = 1$, $v_f = 1$, on the domain $[0,1]$. The initial

and boundary conditions are $\rho(x, 0) = 0$, for all $x \in [0, 1]$ and $\rho(0, t) = 0.47$ for $t > 0$. The solution obtained from this configuration is a rarefaction wave, expressed as

$$\rho(x, t) = \begin{cases} 0.47, & \text{for } x \leq 0.06t, \\ \frac{1}{2} - \frac{x}{2t}, & \text{for } 0.06t < x < t, \\ 0, & \text{for } x \geq t. \end{cases}$$

In the context of the motivating biological application, this example models the case where the DNA strand is initially empty since the initial density is zero. The boundary condition indicates that the initiation process begins immediately with RNAPs initiating on the strand at a constant rate so that the density at $x = 0$ is fixed at $\rho(0, t) = 0.47$.

We use $P1$ elements for our Algorithm 2.2 without time filtering. We also set $h = \frac{1}{128}$, $\Delta t = 10^{-4}$, and $\delta = \sqrt{h}$. Figures 1a and 1b show simulations at times $t = 0.5$ and $t = 1$ based on different values of the stabilization parameter χ .

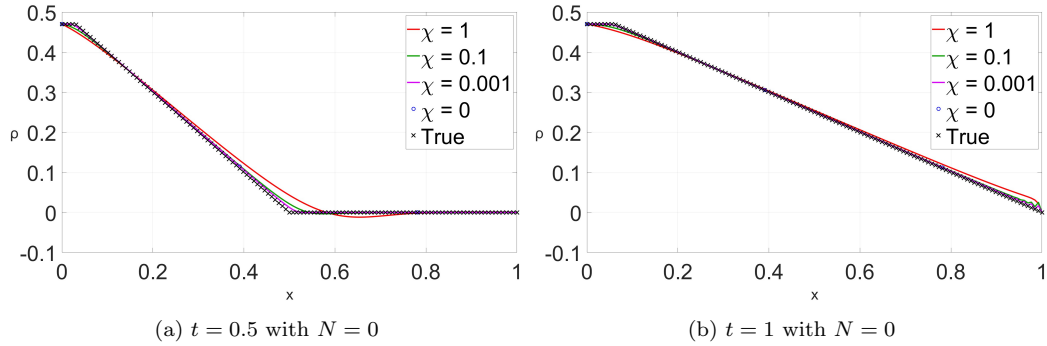


Figure 1: Rarefaction density profile for various χ

As can be somewhat seen in Figures 1a and 1b, the finite element density profile begins to diverge from the true density profile as χ increases.

Figures 2a-2d examine the L^2 error further by plotting $\|\rho_h(\cdot, t) - \rho(\cdot, t)\|$ over time for order of deconvolution $N = 0$ and $N = 1$, combined with $P1$ and $P2$ elements respectively. We observe that the errors for $N = 1$ are smaller than the errors for $N = 0$. Moreover, very small values of χ for stabilization or *no* stabilization yield the best accuracy for the rarefaction solution. This is to be expected, as the rarefaction solution is continuous. In the next section, we will see an example of a discontinuous solution that enjoys the effects of stabilization.

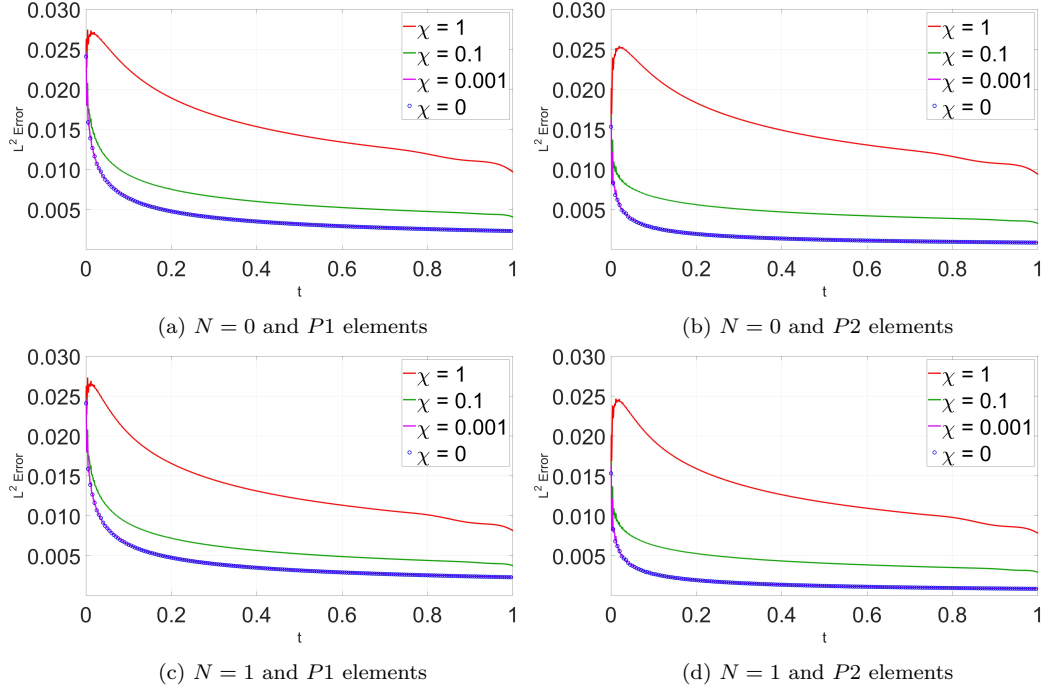


Figure 2: Plots of error in $\|\cdot\|_2$ over time

4.3. Shock Wave

Herein, we explore a shock wave solution to (1) on the domain $[0, 1]$. The parameters $\rho_m = 1$ and $v_f = 1$. We impose boundary and initial conditions $\rho(x, 0) = \frac{1}{3}$ on $(0, 1]$, $\rho(0, t) = \frac{1}{4}$. The shock wave is

$$\rho(x, t) = \begin{cases} \frac{1}{4} & \text{if } x \leq \frac{5}{12}t, \\ \frac{1}{3} & \text{if } x > \frac{5}{12}t. \end{cases}$$

In the context of the biological application, this example corresponds to the case where the strand is initially occupied by RNAPs so that, on average, one third of it is being transcribed. As time moves forward, the initiation rate is decreased so that the density at the initiation site is maintained at $\rho(0, t) = \frac{1}{4}$. The result is a travelling shock wave with a discontinuity that propagates across the domain with shock speed of $\frac{5}{12}$.

We use Algorithm 2.2 without time filtering, with order of deconvolution $N = 0$ and $N = 1$, combined with $P1$ and $P2$ elements. Furthermore, $h = \frac{1}{128}$, $\Delta t = 10^{-4}$, and $\delta = \sqrt{h}$. Figures 3a-3h showcase how adjusting the

stabilization parameter affects the finite element solution for the shock wave problem. The advantage of Vreman stabilization is evident in each of these figures, as increasing χ transforms the finite element solution from a highly oscillatory graph to a smooth shock wave. Additionally, we observe that for a fixed degree of finite elements, increasing the order of deconvolution N does not visibly improve the oscillations. On the other hand, for both $N = 1$ and $N = 2$, increasing the degree of polynomials from $P1$ to $P2$ finite elements reduces the oscillations.

5. Conclusion

After deriving numerical algorithms for the LWR model with Green-shield's velocity, stability and convergence results were presented. Computational simulations supported these results while delivering insights on the behavior of solutions to these algorithms. For instance, the nature of shockwave solutions were captured with Vreman stabilization, while omitting stabilization resulted in spurious oscillations.

It has been shown that the spatial and temporal rates of convergence can be improved with the use of Vreman stabilization and time filtering, respectively. Additionally, we get a better look at the dependence of solutions to Algorithms 2.1 and 2.2 on the order of deconvolution, degree of finite element space, amount of stabilization, and other numerical parameters. Thus, coupling the model with Vreman stabilization and time filtering can serve as a robust model for density profiles of RNA polymerase transcription, which can yield implications about protein synthesis.

6. Acknowledgements

The contribution of authors, Dr. Davis and Dr. Pahlevani, was supported by the National Science Foundation under Awards DMS-1951510 and DMS-1951563. Any opinions, findings, and conclusions or recommendations expressed in this material are those of the author(s) and do not necessarily reflect the views of the National Science Foundation.

References

- [1] L. Davis, M. Neda, F. Pahlevani, J. Reyes, J. Waters, A numerical study of a stabilized hyperbolic equation inspired by models for

- bio-polymerization, *Computational Methods in Applied Mathematics* (2024).
- [2] L. Davis, F. Pahlevani, T. S. Rajan, An accurate and stable filtered explicit scheme for biopolymerization processes in the presence of perturbations, *Applied and Computational Mathematics* 10 (2021) 121–137.
 - [3] L. Davis, T. Gedeon, J. Gedeon, J. Thorenson, A traffic flow model for bio-polymerization processes, *Journal of Mathematical Biology* 68 (2014) 667 – 700.
 - [4] B. D. Greenshields, A study of traffic capacity, in: *Proceedings of the highway research board*, volume 14, 1935, pp. 448–477.
 - [5] A. A. Dunca, M. Neda, On the Vreman filter based stabilization for the advection equation, *Applied Mathematics and Computation* 269 (2015) 379–388.
 - [6] A. Vreman, The filtering analog of the variational multiscale method in large-eddy simulation, *Physics of Fluids* 15 (2003) L61–L64.
 - [7] A. Guzel, W. Layton, Time filters increase accuracy of the fully implicit method, *BIT Numerical Mathematics* 58 (2018) 301–315.
 - [8] V. Decaria, W. Layton, H. Zhao, A time accurate, adaptive discretization for fluid flow problems, *International journal of numerical analysis and modeling* 17 (2020).
 - [9] K. Boatman, L. Davis, F. Pahlevani, T. S. Rajan, Numerical analysis of a time filtered scheme for a linear hyperbolic equation inspired by DNA transcription modeling, *Journal of Computational and Applied Mathematics* 429 (2023) 115135.
 - [10] M. Germano, Differential filters of elliptic type, *The Physics of fluids* 29 (1986) 1757–1758.
 - [11] C. C. Manica, S. K. Merdan, Finite element error analysis of a zeroth order approximate deconvolution model based on a mixed formulation, *Journal of mathematical analysis and applications* 331 (2007) 669–685.

- [12] L. Berselli, T. Iliescu, W. Layton, Mathematics of large eddy simulation of turbulent flows, Scientific Computation, Springer-Verlag, Berlin, 2006.
- [13] A. Dunca, Y. Epshteyn, On the Stolz–Adams deconvolution model for the large-eddy simulation of turbulent flows, SIAM Journal on Mathematical Analysis 37 (2006) 1890–1902.
- [14] W. Layton, C. C. Manica, M. Neda, L. G. Rebholz, Numerical analysis and computational testing of a high accuracy Leray-deconvolution model of turbulence, Numerical Methods for Partial Differential Equations: An International Journal 24 (2008) 555–582.
- [15] W. J. Layton, L. G. Rebholz, Approximate deconvolution models of turbulence: analysis, phenomenology and numerical analysis, volume 2042, Springer Science & Business Media, 2012.
- [16] W. J. Layton, C. C. Manica, M. Neda, L. G. Rebholz, Helicity and energy conservation and dissipation in approximate deconvolution LES models of turbulence, Advances and Applications in Fluid Mechanics 4 (2008) 1–46.
- [17] J. Connors, W. Layton, On the accuracy of the finite element method plus time relaxation, Mathematics of computation 79 (2010) 619–648.
- [18] S. Brenner, L. Scott, The Mathematical Theory of Finite Element Methods, Springer, 2008.
- [19] M. D. Gunzburger, Finite element methods for viscous incompressible flows: a guide to theory, practice, and algorithms, Elsevier, 2012.
- [20] J. G. Heywood, R. Rannacher, Finite-element approximation of the non-stationary Navier-Stokes problem. Part IV: Error analysis for second-order time discretization, SIAM J. Numer. Anal. 27 (1990) 353–384.
- [21] S.-K. Kang, Y.-H. Kwon, A nonlinear Galerkin method for the Burgers equation, Communications of the Korean Mathematical Society 12 (1997) 467–478.
- [22] J. Shen, R. Temam, Nonlinear Galerkin method using Chebyshev and Legendre polynomials I. the one-dimensional case, SIAM journal on numerical analysis 32 (1995) 215–234.

- [23] L. Davis, F. Pahlevani, T. Susai Rajan, An accurate and stable filtered explicit scheme for biopolymerization processes in the presence of perturbations, *Applied and Computational Mathematics* 10 (2021) 121–137. doi:10.11648/j.acm.20211006.11.

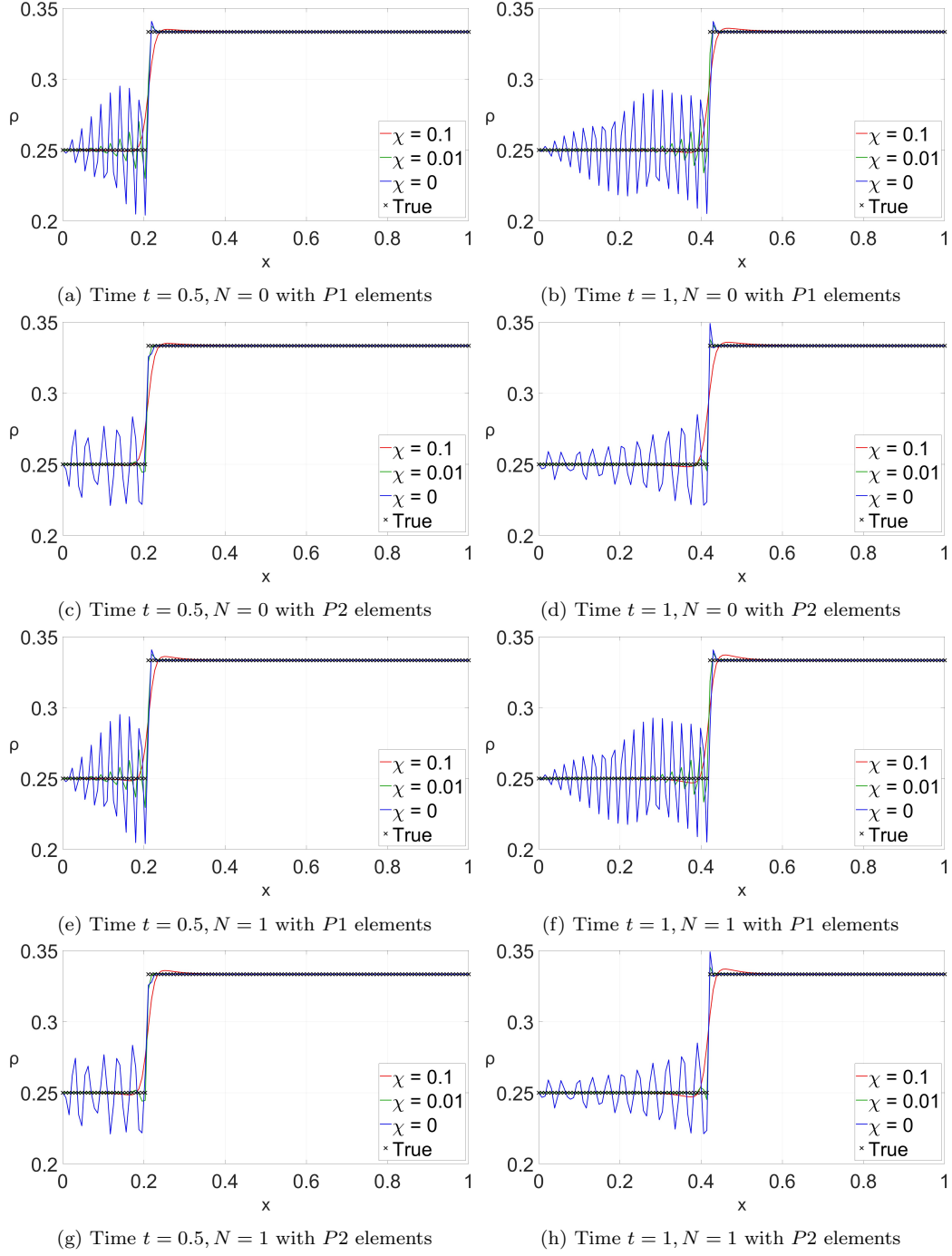


Figure 3: Shock wave density profiles for various values of χ

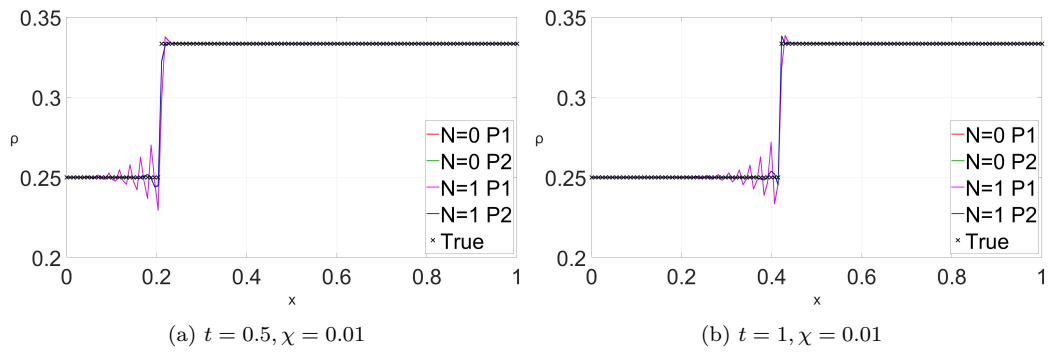


Figure 4: Shock wave density profiles for various combinations of N, k